

Direct Production of Porous Cathode Material ($\text{La}_{1-x}\text{Sr}_x\text{MnO}_3$) Using a Reactive DC Thermal Plasma Spray System

Hyun-Ki Kang and Patrick R. Taylor

(Submitted 12 September 2000)

The cathode material ($\text{La}_{0.8}\text{Sr}_{0.2}\text{MnO}_3$) in solid oxide fuel cells (SOFCs) was plasma sprayed on mild steel in a reactive DC thermal plasma spray process. This high-speed process of depositing thin films for the components of SOFCs was examined experimentally. The results showed that a coating layer of $\text{La}_{0.8}\text{Sr}_{0.2}\text{MnO}_3$ with a particular porosity could be obtained directly using both prereacted $\text{La}_{0.8}\text{Sr}_{0.2}\text{MnO}_3$ and mixed raw materials (La_2O_3 , SrCO_3 , and MnO or MnCO_3) as feed materials with or without a pore former. The heat treatment of the plasma coating material at 1073 K (800 °C) for 3 h significantly enhanced the desired crystallization of $\text{La}_{0.8}\text{Sr}_{0.2}\text{MnO}_3$ in the coated material.

Keywords cathode material, DC plasma spray, heat treatment, high-speed process

1. Introduction

Strontium-doped lanthanum manganite ($\text{La}_{1-x}\text{Sr}_x\text{MnO}_3$) has been extensively studied as a cathode material in the solid oxide fuel cell (SOFC) due to high electrical conductivity, adequate compatibility with Y_2O_3 -stabilized ZrO_2 (YSZ) electrolytes, and an acceptable thermal expansion coefficient compared to other cell components.^[1-5] Various methods such as slurry coating, flame spray, tape casting, and thin film depositions have been used for the fabrication of $\text{La}_{1-x}\text{Sr}_x\text{MnO}_3$ cathodes. Conventional ceramic methods used for the synthesis of these powders include several repeated steps of grinding and sintering.

At present, the central SOFC component, the membrane-electrode assembly, is fabricated by time-consuming sintering methods, which include tape casting,^[6] screen printing,^[7,8] and cofiring^[9] of porous electrodes consisting of a perovskite-type ($\text{La,Sr})\text{MnO}_3$ and a YSZ/Ni cermet, respectively.

Present plasma-spraying methods^[5,10] use a prereacted $\text{La}_{1-x}\text{Sr}_x\text{MnO}_3$ powder, which is calcined at 1673 K (1400 °C) for 3 h and then ground and sieved. A pore former is sprayed with the powder to produce porous cathode layers in SOFCs. The method described here may contribute to the reduction of the production cost of SOFCs compared to conventional technology. The proposed plasma spray method uses a mixture of powders of La_2O_3 , SrCO_3 , and MnCO_3 to produce a porous $\text{La}_{1-x}\text{Sr}_x\text{MnO}_3$ cathode layer directly. In addition, this DC plasma spray method uses argon instead of helium as the plasma gas and carrier gas, further reducing the cost of production, and

does not require the addition of pore formers. In the present study, a direct synthesis process of $\text{La}_{1-x}\text{Sr}_x\text{MnO}_3$ thin films using raw materials (La_2O_3 , SrCO_3 , and MnCO_3) in a reactive thermal plasma spray process was developed.

2. Experimental

Starting powders of La_2O_3 (Johnson-Matthey (Ward Hill, MA), >99.9%, 325 mesh), SrCO_3 (Johnson-Matthey (Ward Hill, MA), >97.5%, 325 mesh), and MnCO_3 (Johnson-Matthey (Ward Hill, MA), >99%, 325 mesh) were mixed in stoichiometric proportions to obtain $\text{La}_{0.8}\text{Sr}_{0.2}\text{MnO}_3$. The powders were mixed and ground by hand using an agate mortar and pestle for 20 min. This powder was dried for 10 h at 353 K (80 °C) in an electric muffle furnace and sieved using a standard 325 mesh to achieve consistent powder feeding and a resultant uniform coating. This powder was fed into the plasma spray gun from a powder feeder and plasma sprayed onto a sandblasted mild steel substrate ($33 \times 45 \times 4 \text{ mm}^3$). The experimental setup is shown in Fig. 1. Table 1 shows the operating parameters for the plasma spray system. Heat treatment was performed at 1073 K (800 °C) for 3 h in air at a heating rate of 7 K/min. Argon was used as both plasma and carrier gas.

For comparison, prereacted $\text{La}_{0.8}\text{Sr}_{0.2}\text{MnO}_3$ was prepared by a conventional solid-state reaction using a stoichiometric mixture of La_2O_3 , SrCO_3 , and MnO held at 1673 K (1400 °C) for 3 h in an air atmosphere. The calcined powder was ground in an agate mortar and sieved using a standard 325 mesh screen. This powder was blended with 5 wt.% carbon black (−200 mesh) as a pore former and was plasma sprayed on sandblasted mild steel ($33 \times 45 \times 4 \text{ mm}^3$).

The morphology of the powder and the microstructure of the coated cathode layer were analyzed by scanning electron microscopy (SEM, Hitachi, 2400). The phase compositions of the powder and coated layer were characterized by x-ray diffraction (XRD, $\text{Cu } K_\alpha$). The different experimental procedures between the two processes are shown in Fig. 2.

Hyun-Ki Kang, Department of Materials, Metallurgical, Mining and Geological Engineering, The University of Idaho, Moscow, ID 83844-3024; and Patrick R. Taylor, Department of Materials Sciences & Engineering, The University of Tennessee, Knoxville, TN 37996-2200. Contact e-mail: prtaylor@utk.edu.

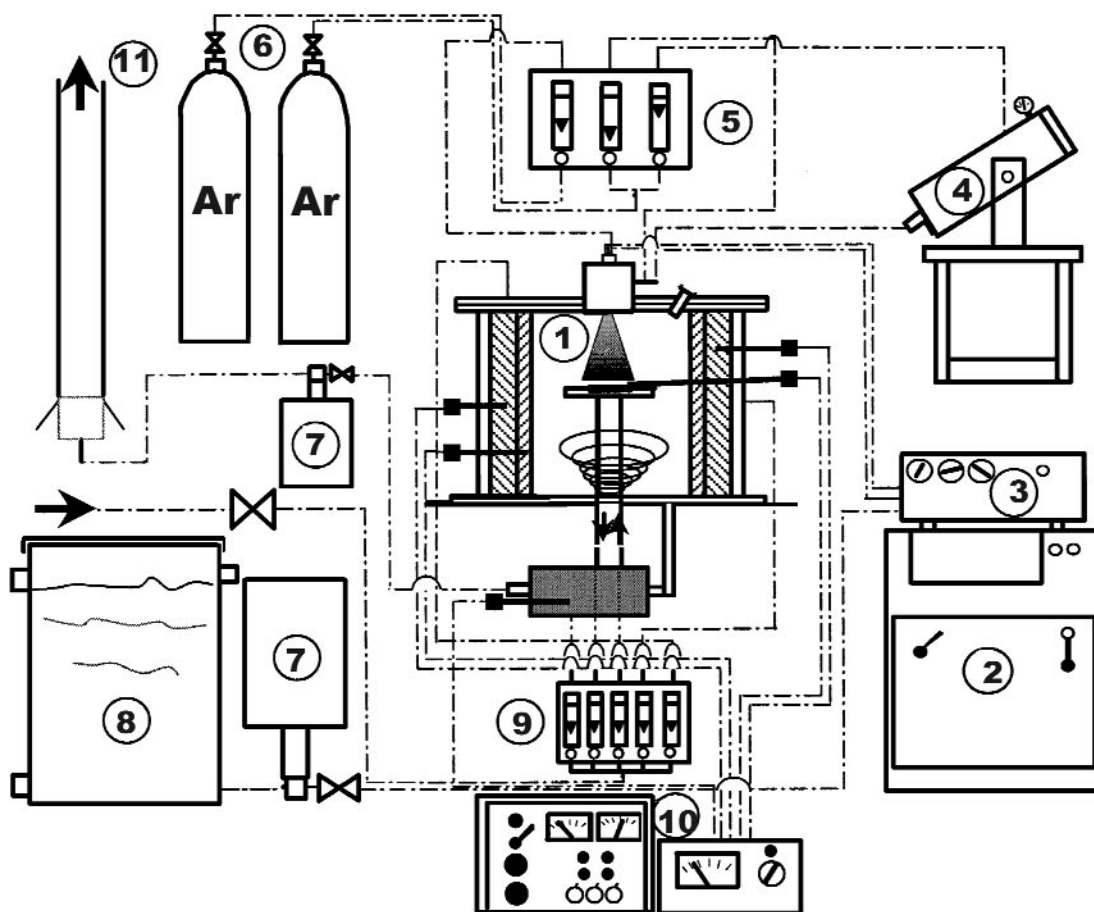


Fig. 1 System sketch: (1) reactor, (2) power supply, (3) arc starter, (4) powder feeder, (5) gas flow meter, (6) fuel and carrier gas, (7) fan and water pump, (8) water tank, (9) water flow meter, (10) control panel and thermometer, and (11) exit pipe

Table 1 Equipment and parameters of the Miller DC plasma spray

Equipment	Parameters
Plasma spray power supply: PS-100	Plasma arc current: 700–1050 A
High-frequency arc starter: HF-2200	Plasma arc voltage: 31–38 V
Operation control: PC-100R	Arc gas: 345 kPa Ar
Cathode: 1083-720, 80 kW	Carrier gas: 207 kPa Ar
Anode: 2083-730, 40 kW	Powder feeding rate: 2 g/min
Gas injector: 3083-112, 40 kW	Standoff distance: 90–145 mm

3. Results and Discussion

3.1 XRD Analysis

Preliminary experiments using the mixtures La_2O_3 , SrCO_3 , and MnO were carried out in the reactive thermal plasma system at different input powers, but under the same powder feeding rate (2 g/min) and standoff distance (145 mm). A trend is apparent that increasingly stronger $\text{La}_{0.8}\text{Sr}_{0.2}\text{MnO}_3$ peaks can be obtained gradually (with a decrease in the lanthanum oxide phase) as input power is increased, as shown in Fig. 3. The manganese oxide phase remains almost the same. In these mixtures, the

manganese oxide particle size (+200 mesh) is larger than that in the other precursors (−325 mesh).

Figure 4 shows that a significant improvement of crystallization of $\text{La}_{0.8}\text{Sr}_{0.2}\text{MnO}_3$ was obtained after heat treatment of the sample. Although heat treatment enhanced the chemical reaction, some impurities (La_2O_3 , SrO , and MnO) exist in the powder.

Figure 5 shows that a shorter standoff distance (at an input power of 35 kW) improved the chemical reaction due to a higher heat flux. In addition, a shorter standoff distance increased the rate of deposition on the substrate.

3.2 Microstructure

For solid oxide fuel cell applications, 30 to 40% porosity in the electrodes is generally required. Figure 6(a) and (b) show a porous coating of plasma-sprayed material from prereacted $\text{La}_{0.8}\text{Sr}_{0.2}\text{MnO}_3$, 325 mesh, 1673 K (1400 °C) for 3 h, mixed with 5 wt.% carbon black. Completely melted coating layers were observed at an input power of 23 kW, but inhomogeneous pores were found because the carbon black could not be homogeneously mixed with the coarse $\text{La}_{0.8}\text{Sr}_{0.2}\text{MnO}_3$. Microstructures of the as-sprayed coating directly from raw materials (La_2O_3 , SrCO_3 , and MnCO_3) are shown in Fig. 6(c) and (d). The pore dis-

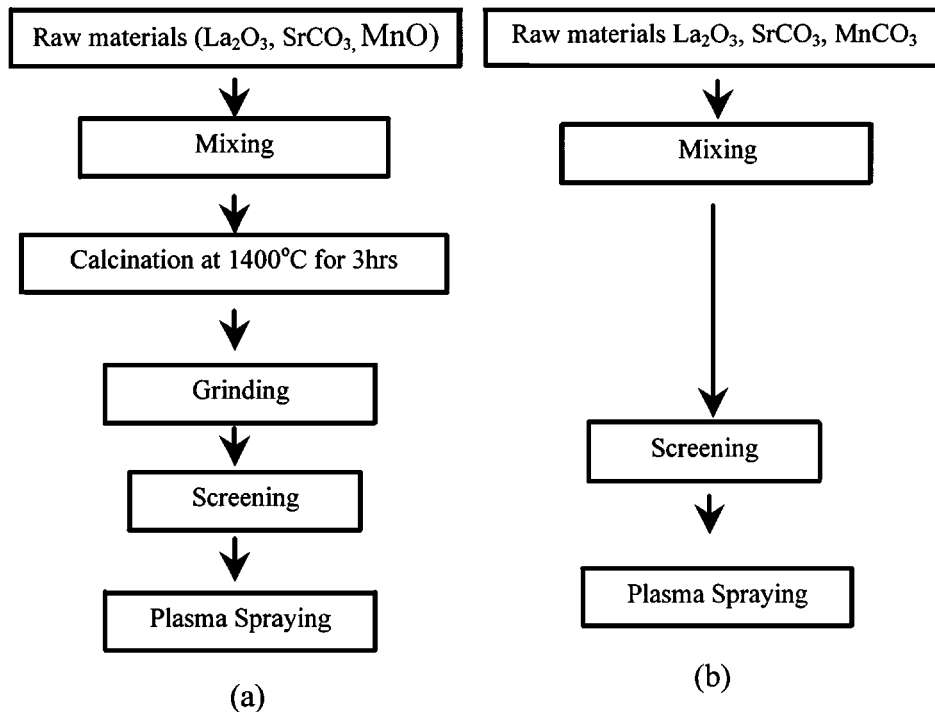


Fig. 2 (a) Current plasma spray and (b) reactive plasma spray processes

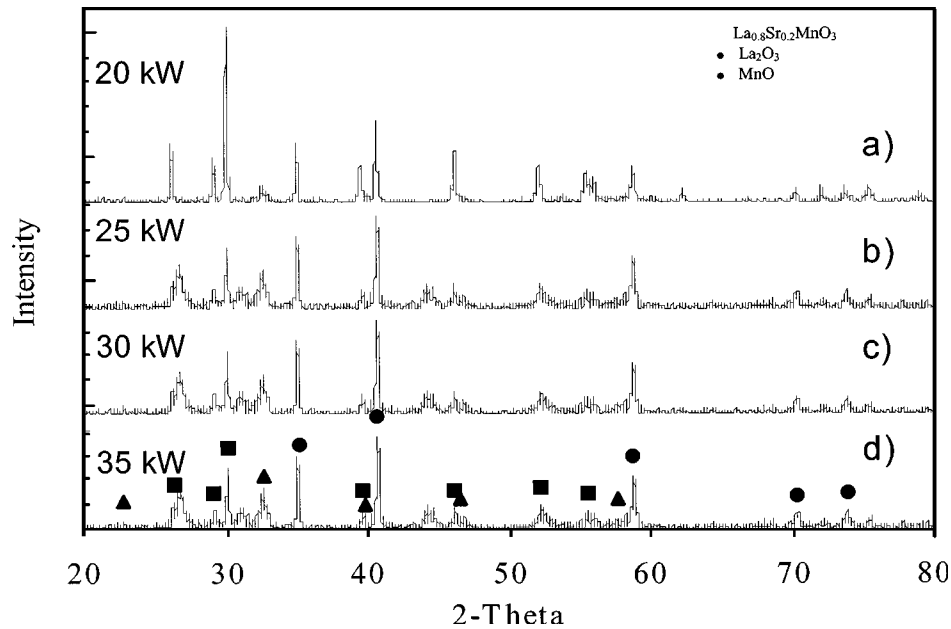


Fig. 3 (a) to (d) XRD for plasma-sprayed 0.4La₂O₃ + 0.2SrCO₃ + MnCO₃ under different input powers

tribution appears to be better than those of prereacted La_{0.8}Sr_{0.2}MnO₃ (Fig. 6a and b).

Unmelted particles were found at an input power of 35 kW in Fig. 6(c), and it is believed that lanthanum oxide was melted par-

tially in a plasma flame due to its higher melting temperature of 2595 K compared to the other materials. Figure 6(e) shows that bonding between the coating layer and the sandblasted substrate is good and that the thickness of the coating layer is around 1 mm.

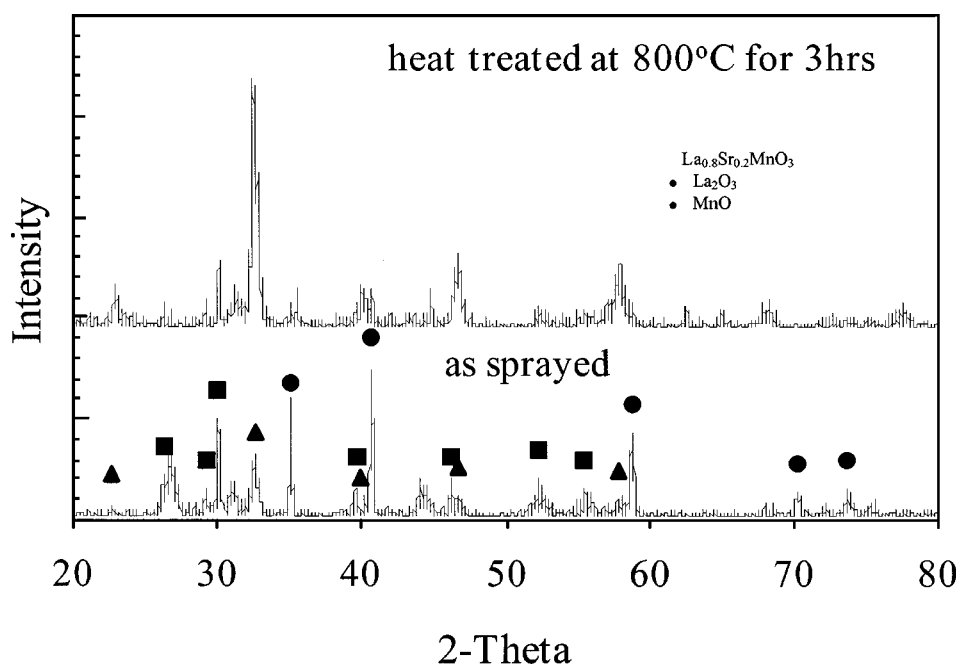


Fig. 4 XRD for plasma-sprayed $0.4\text{La}_2\text{O}_3 + 0.2\text{SrCO}_3 + \text{MnCO}_3$ at 30 kW

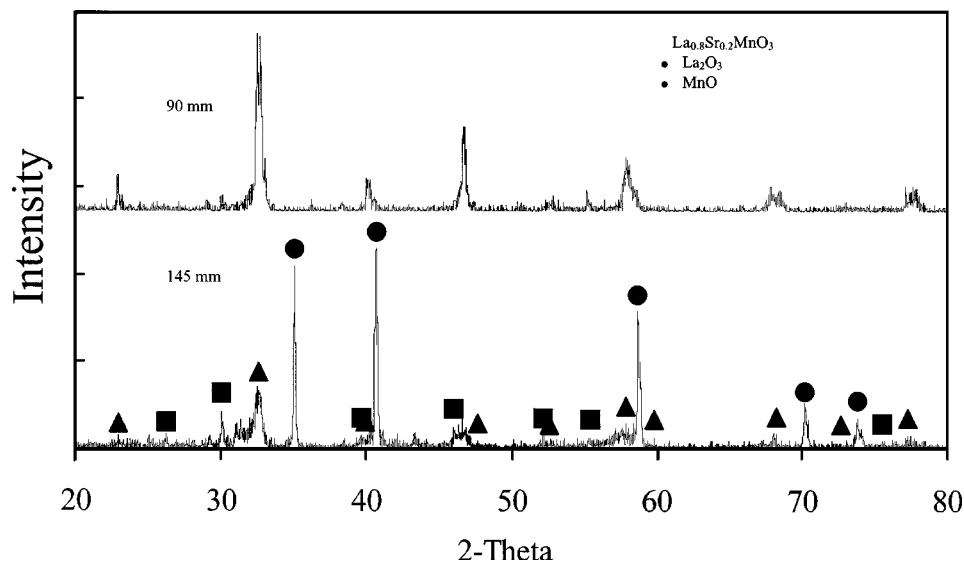


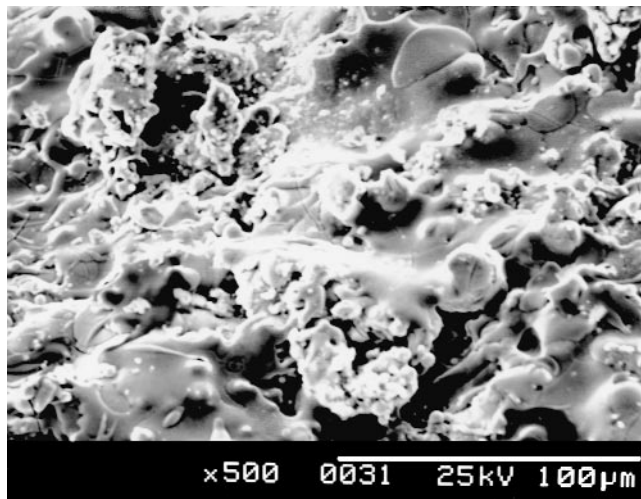
Fig. 5 XRD for plasma-sprayed $0.4\text{La}_2\text{O}_3 + 0.2\text{SrCO}_3 + \text{MnCO}_3$ at different standoff distances

4. Conclusions

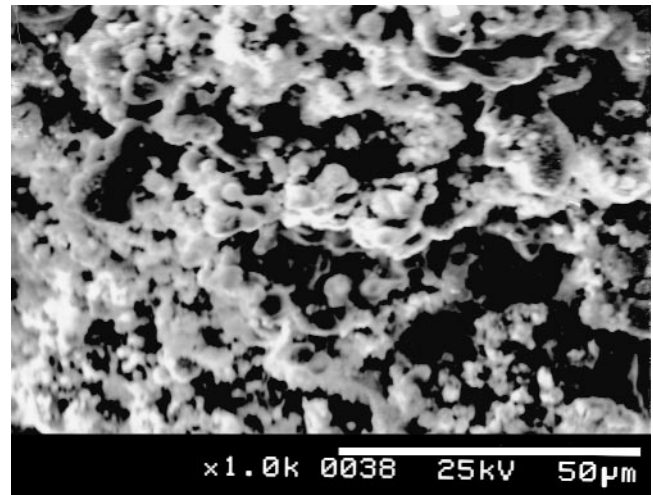
A $\text{La}_{0.8}\text{Sr}_{0.2}\text{MnO}_3$ film was produced using both raw materials (La_2O_3 , SrCO_3 , and MnCO_3) and prereacted $\text{La}_{0.8}\text{Sr}_{0.2}\text{MnO}_3$ as precursors in a reactive DC thermal plasma spray system. Very small amounts of lanthanum oxide exist in the coating layer at an input power of 35 kW and a standoff distance of 90 mm when spraying the raw materials (La_2O_3 , SrCO_3 , and

MnCO_3). Spraying prereacted $\text{La}_{0.8}\text{Sr}_{0.2}\text{MnO}_3$ with 5 wt.% carbon black produced larger and less homogeneous pores than did spraying with a mixture of La_2O_3 , SrCO_3 , and MnCO_3 .

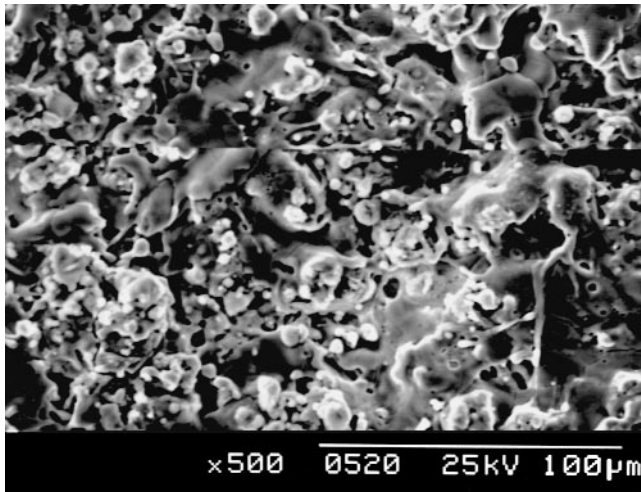
Heat treatment at 1073 K (800 °C) for 3 h enhanced the chemical reaction. In the case of the mixture of La_2O_3 , SrCO_3 , and MnO , manganese oxide impurities were detected even though the input power was increased up to 35 kW to compensate for the larger manganese oxide particle size (+200 mesh).



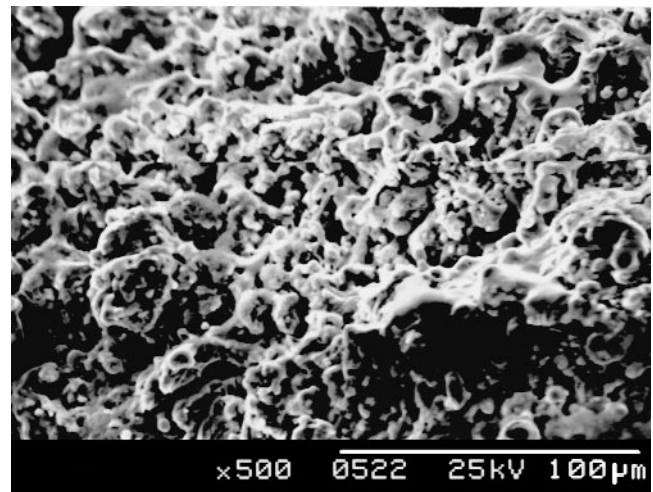
(a)



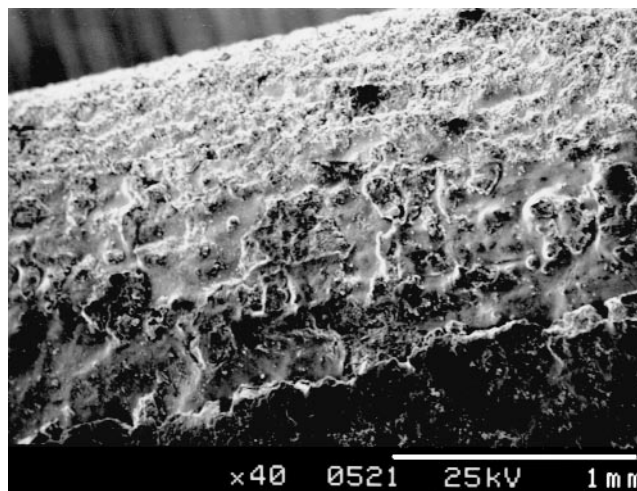
(b)



(c)



(d)



(e)

Fig. 6 SEM micrographs of porous coating from heat-treated lanthanum strontium manganite (LSM): (a) top view and (b) side view; and La_2O_3 , SrCO_3 , and MnCO_3 : (c) top view, (d) side view), and (e) bonding layer

Through experimentation, $\text{La}_{0.8}\text{Sr}_{0.2}\text{MnO}_3$ was formed as a major phase with small amounts of impurities.

References

1. G. Schiller and M. Müller: in *United Forum Scientific Technological Advances*, C.C. Berndt, ed., ASM International, Materials Park, OH, 1997, pp. 349-52.
2. Feng Zheng and Larry R. Pederson: *J. Electrochem. Soc.*, 1999, vol. 146 (8), pp. 2810-16.
3. Z. Li, W. Mallener, L. Fuerst, and D. Stöver: in *Thermal Spray Research, Design and Applications*, C. C. Berndt and T.F. Bernecki, eds., ASM International, Materials Park, OH, 1993, pp. 343-46.
4. R.N. Basu, S.M. Pratihari, and H.S. Mati: *Materials Letters*, Elsevier Science B.V., Amsterdam, Netherlands, 1997, vol. 32 (4), pp. 217-22.
5. G. Schiller, R. Henne, and M. Lang: *Proc. 5th Int. Symp. on Solid Oxide Fuel Cell (V)*, U. Stimming, S. C. Singhal, H. Tagawa, and W. Lehnert, eds., The Electrochemical Society, Pennington, NJ, 1997, pp. 635-41.
6. K. Honegger, E. Batawi, C. Sprecher, and R. Diethelm: *Proc. 5th Int. Symp. on Solid Oxide Fuel Cell (V)*, U. Stimming, S. C. Singhal, H. Tagawa, and W. Lehnert, eds., The Electrochemical Society, Pennington, NJ, 1997, p. 321.
7. M. Kuznecov, P. Otschik, K. Eichler, and W. Schaffrath: *Proc. 5th Int. Symp. on Solid Oxide Fuel Cell (V)*, U. Stimming, S. C. Singhal, H. Tagawa, and W. Lehnert, eds., The Electrochemical Society, Pennington, NJ, 1997, p. 907.
8. Gwi-Yeol Kim, Seung-Wook Eom, and Seong-In Moon: *Proc. 5th Int. Symp. on Solid Oxide Fuel Cell (V)*, U. Stimming, S. C. Singhal, H. Tagawa, and W. Lehnert, eds., The Electrochemical Society, Pennington, NJ, 1997, p. 701.
9. Suk Woo Nam, Seung-Ahn Hong, and Il-Young: *Proc. 5th Int. Symp. on Solid Oxide Fuel Cell (V)*, U. Stimming, S. C. Singhal, H. Tagawa, and W. Lehnert, eds., The Electrochemical Society, Pennington, NJ, 1997, p. 293.
10. R. Henne, G. Schiller, V. Borck, and M. Mueller: *Thermal Spray: Meeting the Challenges of the 21st Century*, C. Coddet, ed., ASM International, Materials Park, OH, 1997, pp. 933-38.

